Bulit-in self-test and calibration for electrostatic MEMS gyroscope based-on voltage controlled oscillator

Elaf Talib Nayel
Department of Electrical Engineering
College of Engineering
University of Babylon
Iraq
eng774.elaf.talib@student.uobabylon.edu.iq

Qais Al-Gayem
Department of Electrical Engineering
College of Engineering
University of Babylon
Iraq
eng.qais.karem@uobabylon.edu.iq

Abstract— This work aims to improve Electrostatic MEMS vibratory gyroscope dependability by developing methods. The not control stiffness changes which occur due to different environmental and operational conditions. The proposed system uses a closed-loop control structure with a VCO-based self-test and calibration mechanism to monitor stiffness-related frequency shifts and restor the degraded response. The system uses Voltage-Controlled Oscillator (VCO) technology to track resonant frequency changes which serve as direct evidence of stiffness variations. Simulation results in MATLAB/Simulink demonstrate that the proposed design effectively detects stiffness reductions and applies real-time calibration. The proposed calibration method achieved 99.3% ferquency recovery with a residual error od about 30Hz and approimately 95% stiffness recovery, demonstrating the effectiveness of the proposed compensation loop.

Keywords— MEMS Gyroscope, Electrostatic Actuation, Stiffness Degradation, Self-test, Online Calibration, AGC, PLL.

I. Introduction

Microelectromechanical Systems (MEMS) gyroscopes have emerged as critical components in various modern applications, ranging from consumer electronics to high-precision navigation systems. However, their reliability is frequently challenged by environmental factors and operational stresses, such as temperature fluctuations and mechanical wear for both industrial and consumer applications [1].

Modern MEMS gyroscopes employ closed-loop control techniques to improve stability and maintain reliable operation, However, parameter variations such as stiffness and mass changes can still affect the resonant behavior of the system. Therefore, monitoring the resonant frequency provides an effective approach for detecting struchural degradation in MEMS fyroscope [2-3].

There for the MEMS gyroscope systems still need long-term operational reliability solutions. The performance degradation mechanisms which exist through drift and structural stress and material changes will progressively diminish the sensor dynamic performance over an extended operational period [4]. This work investigates infiuence of mechanical parameter variations, including stiffness, mass, damping changes, on the behavior of a closed-loop MEMS gyroscope. A simulation-based framework is proposed to investing degradation caused by parameter variations while developing a frequency-based self-test method. So, this work aims to analyze parameter-induced degradation in closed-loop MEMS gyroscope and to develop a parameter-based analysis and frequency-based self-test method capable of detecting mechanical parameter variations in MEMS gyroscope [5].

II. Operation Principle and Mathematical Model of the Electrostatic MEMS gyroscope

The electrostatic MEMS gyroscope operates according to its dynamic behavior. The vibrating system operates as a second-order dynamic system.

$$m\ddot{x} + c\dot{x} + kx = F(t) \quad (1)$$

where m is the effective mass, c is the damping coefficient, k is the stiffness, and F(t) represents the applied excitation force.

The electrostatic actuation force generated by the drive voltage is expressed as:

$$F_{elec} = \frac{1}{2}\frac{\partial C}{\partial x} V^2 \quad (2)$$

Where (∂C) / (∂×) is the capacitance gradient, and V is the applied drive voltage.

In the sense axis, the Coriolis force acts as the input excitation, Fc is defined by the equation:

$$Fc = 2m\Omega\dot{x}) \quad (3)$$

where **Ω** is the applied angular velocity, and ẋ is the drive-axis velocity.

In the Laplace domain, the mechanical dynamics can be expressed by the transfer function from the excitation force F(s) to the displacement X(s) as:

$$G(s)=x(s)/F(s) = 1 / (m\ s\text{^}2+cs+k) \quad (4)$$

Where m is the effective mass, c is the damping coefficient, and k is the stiffness of the resonant structure.

The natural resonant frequency of the mechanical structure is determined by the system parameters, Wn is the natural angular frequency of the resonant is defined in the equation:

$$Wn = \sqrt{(k/m)} \quad (5)$$

The corresponding resonant frequency in hertz is defined in equation:

$$Fn = 1/2\ \pi\ \sqrt{(k/m)} \quad (6)$$

Therefore, any reduction in stiffness k leads to a proportional decrease in the resonant frequency, making the frequency shift Δf a reliable indicator of structural degradation.

Any change in the mechanical parameters m, k, directly affects the resonant frequency and dynamic response of the system [6].

The aging effects, material fatigue, contamination, temperature stress, and stress of practical MEMS gyroscopes lead to progressive changes in their stiffness, mass, and damping properties [7].

III. CLOSED-LOOP CONTROL ARCHITECTURE

The closed-loop drive control architecture is used to maintain a stable vibration amplitude in the MEMS gyroscope. The feedback signal continuously adjusts the drive input to compensate for parameter variations such as mass, damping, and stiffness variations [8]. To achieve maximum vibration response, the operating frequency was established at the resonant frequency which was calculated to be 4.56 kHz ($w_n \approx 28636$ rad/s) [9].

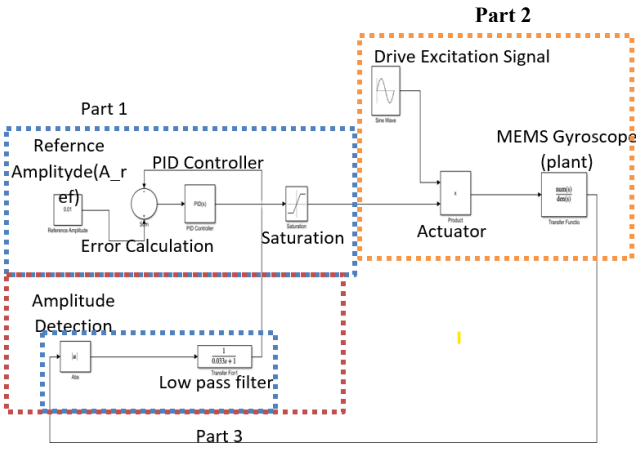

Figure 1: Simulink model of the closed-loop drive control system of the electrostatic MEMS gyroscope

A. *Control System*

Part 1 represents the closed-loop control system, where the reference amplitude is compared with the feedback signal to generate an error signal. This error is processed by the controller generate the control signal applied to the actuator.

B. *Excitation & Signal Processing*

Part 2 represents the excitation and signal processing stage, where a sinusoidal signal is generated and combined with the control signal through a multiplier before being applied to the system.

C. *Mechanical Model*

Part 3 represents the mechanical dynamics of the MEMS gyroscope, modeled as a mass–spring–damper system. The output is processed to extract the amplitude, which is fed back to the control loop [10].

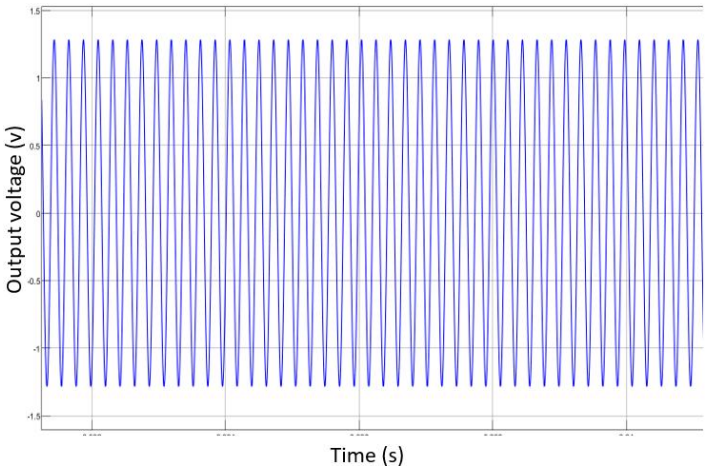

Figure2: Simulated steady-state waveform of the MEMS gyroscope under nominal operating condition.

The waveform in figure 2 a stable resonant oscillation at 4.588 kHz with an amplitude of 1.2 v.

The fault model assessment begins after establishing the nominal response as a baseline reference because the assessment requires gradual stiffness parameter reduction from -1% to -31% to determine its impact on gyroscope output frequency and amplitude.

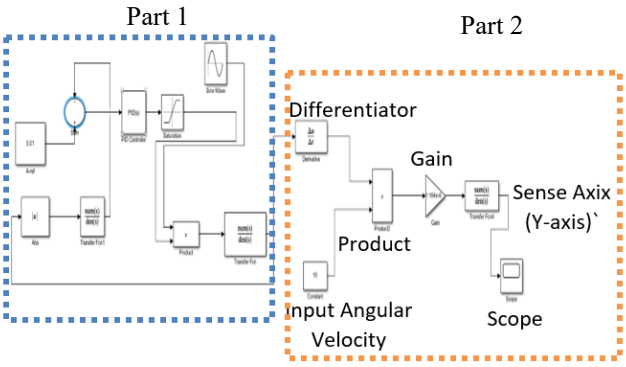

Figure 3: Complete Simulink model of the electrostatic MEMS gyroscope system.

Part 1 represents the drive axis responsible for generating a stable oscillation of the proof mass. In contrast, Part 2 focuses on the sense axis. The displacement signal is differentiated to obtain velocity, then multiplied by the angular rate to generate the Coriolis force.

IV. PARAMETER-BASED FAULT MODELING

To analyze the effect of structural degradation on the MEMS gyroscope performance, faults are simulated by varying the key mechanical parameters of the system, namely mass (m), damping (c), and stiffness (k) [11]. To represent the effect of mechanical fatigue, and thermal stress, a stiffness degradation model is introduced as a gradual reduction in the nominal stiffness value k.

A. *Stiffness Degradation Analysis (K)*

The created a model that showed how stiffness degradation occurred through a progressive decline of the parameter value. The stiffness degradation model was implemented by

reducing the nominal stiffness value according to the degradatio percentage ：

$$K_{deg} = (1 - D)K_{nom} \quad (7)$$

Where K_{nom} is the nominal stiffness, K_{deg} is the degraded damping stiffness value, and D represents the applied degradation percentage fiom -1% to -31%. The effect of on stiffness was studied by decreasing K from -1 % to -31% in 2% intervals while maintaining all other parameters at their original value [12].

Table 1: Effect of stiffness degradation on the resonant frequency of the MEMS gyroscope.

Stiffness (K)	Frequency operation	Resonant Frequency
485.46	4596.9	4557.9
480.61	4596.9	4534.8
470.91	4596.9	4488.7
461.19	4596.9	4442.2
451.48	4596.9	4395.2
441.77	4596.9	4347.7
432.06	4596.9	4299.6
422.35	4596.9	4251.0
412.64	4596.9	4201.9
402.93	4596.9	4152.2
393.22	4596.9	4101.8
383.51	4596.9	4050.9
373.80	4596.9	3999.3
364.10	4596.9	3947.0
354.39	4596.9	3894.0
344.68	4596.9	3840.3
334.97		3785.8

The results confirm that a gradual reduction in stiffness leads to a proportional decrease in the resonant frequency, consistent with, as shown in equation (5,6).

B. Mass Variation Analysis (m)

The variation in the proof mass (m) due to aging, contamination, or material deposition can influence the dynamic behavior of the MEMS gyroscope, (5,6).

The mass degradation model is m_{deg} is expressed as:

$$m_{deg} = (1 - D)m_{nom} \quad (8)$$

Where M_O is the nominal mass and D is the degradation percentage.

The study used controlled mass variations to model aging-related degradation through the Simulink model. The frequency deviation (Δf) data was used to evaluate the sensitivity of the frequency-based self-test mechanism functioned. The research shows that mass-induced frequency shifts allow closed-loop MEMS gyroscope systems to detect faults at an early stage [13].

Table 2: Effect of mass degradation on the resonant frequency of the MEMS gyroscope.

Proof mass (m)	Operation frequency	Resonant Frequency
5.92*10^-7	4566.3	4557.9
5.861*10^-7	4566.3	4580.6
5.742*10^-7	4566.3	4627.5
5.624*10^-7	4566.3	4676.0
5.506*10^-7	4566.3	4726.0
5.387*10^-7	4566.3	4777.7
5.269*10^-7	4566,3	4831.0
5.150*10^-7	4566.3	4886.3
5.032*10^-7	4566.3	4943.4
4.914*10^-7	4566.3	5002.6
4.795*10^-7	4566.3	5064.0
4.677*10^-7	4566.3	5127.7
4.558*10^-7	4566.3	5193.9
4.440*10^-7	4566.3	5262.7
4.322*10^-7	4566.3	5334.1
4.203*10^-7	4566.3	5408.9
4.084*10-7	4566.3	5486.7

The observed trend confirms that resonant frequency decreases as proof mass increases. The mass reduction from -1% to −31% produces an uninterrupted increase in resonant frequency which confirms the theoretical model. The predictable behavior of the system enables to use frequency-based self-test methods for detecting mass loss in resonant MEMS gyroscopes.

C. Damping Variation Analysis

MEMS vibratory gyroscopes experience their effective damping coefficient to rise because of their aging process combined with the environmental degradation processes that affect their operational lifespan. The internal material losses together with surface effects and packaging degradation and vacuum condition changes create new energy dissipation paths which lead to an increase in the damping coefficient. The quality factor (Q) of a system depends on its damping coefficient because higher damping levels reduce Q-factor values which results in lower resonant amplitude. The process of aging leads to higher damping levels while decreasing the oscillation stability for resonant MEMS gyroscopes that operate over extended periods [14].

The damping degradation model is expressed as:

$$C_{deg} = (1 - D)\, C_{nom} \quad (9)$$

Where C_{deg} is the degraded damping factor, C_{nom} is the nominal damping value, and D is the applied degradation percentage.

Table3: Effect of damping coefficient c again on the closed-loop MEMS gyroscope response.

Damping Coefficient (C)	Operation Frequency	Resonant Frequency
1.1830*10^-5	4596.9	4557.6
1.1948*10^-5	4596.9	4557.6
1.2185*10^-5	4596.9	4557.6
1.2422*10^-5	4596.9	4557.6
1.2658*10^-5	4596.9	4557.6
1.2895*10^-5	4596.9	4557.6
1.3131*10^-5	4596.9	4557.6
1.3368*10^-5	4596.9	4557.6
1.3604*10^-5	4596.9	4557.6
1.3841*10^-5	4596.9	4557.6
1.4078*10^-5	4596.9	4557.6
1.4314*10^-5	4596.9	4557.6
1.4551*10^-5	4596.9	4557.6
1.4788*10^-5	4596.9	4557.6
1.5024*10^-5	4596.9	4557.6
1.5261*10^-5	4596.9	4557.6
1.5497*10^-5	4596.9	4557.6

The aging analysis demonstrates that resonant frequency changes occur due to mechanical parameter variations, especially stiffness and mass changes, thus making frequency monitoring a dependable method for detecting structural degradation. Therefore, a frequency-based self-test mechanism is implemented. The time-domain waveform was monitored after stiffness degradation to confirm through visual observation how reduced stiffness affected the gyroscope response. The numerical frequency results showed the actual results from the stiffness testing which included time-domain validation of the testing results.

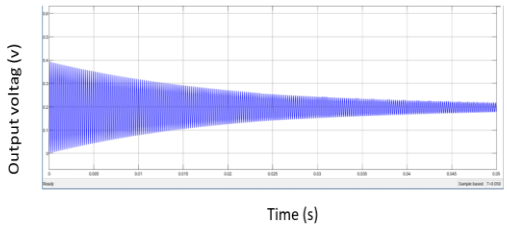

Figure 4: After stiffness degardation, the oscillation amplitude and the related frequency have decreased.

The results shown in Figure 4 demonstrate that when the stiffness coefficient decreases, both the oscillation amplitude and frequency show a clear decline. The degraded gyroscope output showed a damped oscillation pattern which had an envelope frequency of about 40 000 hertz before the self-test circuit was applied. The amplitude measurement decreased from 0.36 to 0.24 which demonstrated how stiffness degradation affected both oscillation energy and transient response.

V. Self-Test

The built-in Self-Test (BIST) system functions as an internal diagnostic method which lets MEMS devices perform self-health assessments without needing external test machines . The system identifies faults in the structure and electronic components and measures how operational performance changes during power-on testing. The VCO output frequency is linearly proportional to the input control voltage and can be expressed as:

$$V_{cc} = f_q + K_n \; V_n \text{.....(10)}$$

Where f_q is the quiescent frequency, K_v is the VCO sensitivity, and V_n is the filtered amplitude input.

The VCO receives the conditioned signal which causes any stiffness-related degradation to result in a matching frequency shift [15].

The enhanced self-test system showed a frequency response that decreased continuously as the stiffness parameter was reduce from -1% to −3% in 2% increments. The research showed that the VCO-based self-test system could detect stiffness degradation through specific frequency shifts which made it useful for both early fault detection and future calibration of closed-loop MEMS gyroscope systems.

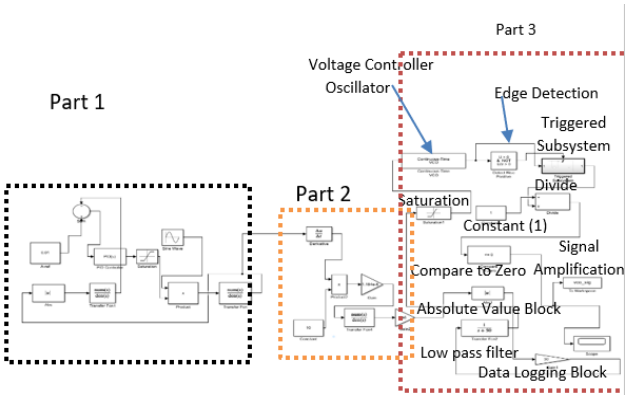

Figure 5: Proposed MEMS gyroscope with VCO_based self-test circuit.

The basic modeling and signal processing elements of the system have been previously descibed in Fig. 1 and Fig.3. The third part represent the VCO-based self-test used to extract the frequency information. The output signal to go through an absolute value block, the vibration envelope. A low-pass filter converts the signal into a DC level the steady-state amplitude of the signal. The VCO system receives the signal which results in amplitude changes from stiffness degradation being converted into frequency variations. The system condition is assessed by monitioring the frequency variation caused by stiffness degradation. The results demonstart that the VCO-based self-test circuit can detect stiffness-related faults through the generated frequency shift, validating the effectiveness of the proposed self-test method. The study demonstrates that the VCO output frequency decreases progressively as stiffness reduction occurs which validates the effectiveness of the new self-testing method. The output frequency of the VCO can be expressed as:

$$f_{vc} = f_o + \; K_n \; V_n \text{.....(11)}$$

where f_o is the quiescent frequency, K_v is the VCO sensitivity, and v_n is the filtered output voltage of the gyroscope. The self-test frequency difference (Δf) was then defined as:

$$\Delta f = f_r - f_{vco} \text{.....(12)}$$

Where f_{vco} is the output frequency, and f_r is the resonant frequency.

Table 4: f_{vco} is the vco output frequency, and f_r is the resonant frequency of the MEMS gyroscope.

Stiffness K (N/m)	Resonant Frequency (Hz)	Δf (Hz)	Δf(%)
485.46	4557.6	0	0
480.61	4534.8	22.8	0.50%
470.90	4488.7	68.9	1.51%
461.19	4442.2	115.4	2.53%
451.48	4395.2	162.4	3.56%
441.77	4347.2	210.4	4.62%
432.06	4299.6	258.0	5.66%
422.35	4251.0	306.6	6.73%
412.64	4201.9	355.7	7.80%
402.93	4152.2	405.4	8.89%
393.22	4101.8	455.8	10.00%
383.51	4050.9	506.7	11.12%
373.80	3999.3	558.3	12.25%
364.09	3947.0	610.6	13.40%
354.39	3894.0	663.6	14.56%
344.68	3840.3	717.8	-15.74%
334.97	3785.8	771.8	16.93%

As presented in Table 4, the VCO operating frequency remained constant at 479.64 Hz, while the resonant frequency decreased progressively with stiffness degradation. The frequency difference Δf showed a monotonic increase with stiffness degradation, confirming that the proposed VCO-based self-test circuit is sensitive to stiffness-related faults and provides a reliable electronic fault eindicator. Confirms that the proposed VCO-based self-test circuit is highly sensitive to stiffness-related faults and provides a reliable electronic fault indicator.

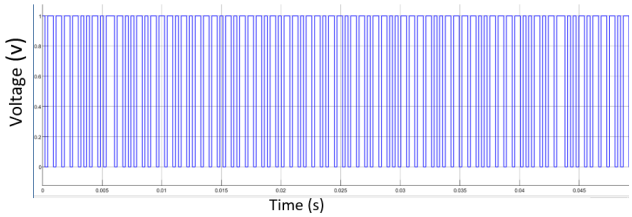

Figure 6: Steady-state VCO pulse train self-test circuit at 1s simulation time.

The VCO output a square pulse train pattern which operates periodically during its steady-state output period. The pulse spacing shows alterations, two factors the VCO control signal ripple and the gyroscope response. The pulse train maintains stability to extract frequencies the self-test circuit's function of converting amplitude signals into frequency signals. The proposed VCO-based self-test circuit generated a square-wave pulse train, confirming the conversion of gyroscope response variations into measurable frequency changes for fault detection.

VI. Calibration Mechanism

The calibration mechanism is required because long-term operation caused parameter variations, such as stiffness degradation,which shift the sensor response from its nominal operating condition. Online compensation is needed to reduce output errors and restore system stability. Calibration methods enable the measurement of gyroscope deviation, which use to restore the instrument's response to its reference state [16-17].

VII. The Calibration Algorithm

The online calibration is designed to compensate for stiffness loss in MEMS gyroscope systems. The frquency shift obtained from the self-test stage is used as an indicator to estimate parameter variations. The variables are defined as follows: K_{est} is the estimated stiffness, ΔK stiffness erorr, K_{nom} nominal stiffness, K_{deg} degraded stiffness, K_{cal} calibration stiffness, and y compensation signal.

$$K_{est} = f(\Delta f) \quad \text{.....(13)}$$

$$\Delta K = K_o - K_{est} \quad \text{.....(14)}$$

$$K_{cal} = K_{deg} + \Delta K \quad \text{.....(15)}$$

$$y = 0.2\, K_{cal} \quad \text{.....(16)}$$

Where K_{deg} estimated stiffness extracted from the self-test frequency shift, ΔK stiffness error, K_{cal} is the calibration stiffness value, K_{deg} degraded stiffness, and y compensation signal applied to the VCO-based calibration loop

The method uses the shift to determine stiffness loss which engineers then use to create a compensation system that brings the sensor back to its regular operational state.

In the calibration loop, the estimated stiffness is sent to a MATLAB Function block to generate the compensation signals requrid to correct the degraded system response. The system used a proportional scaling relationship to create its compensation law, which adjusted the output corrective signal based on the estimated calibration parameter. The VCO stage received the produced signal to use it for restoring the oscillation frequency back to its standard operating level. The final compensation law was implemented as y = 0.2Kcal. The VCO parameters were tuned to a quiescent frequency of 3150 Hz and a sensitivity of 114 Hz/V to achieve stable and fast recovery performance. The proposed calibration loopnrestored the output frequency close to its nominal operating value after stiffness degradation. The gyroscope results showed that the proposed loop achieved approximately 99.3% ferquency recovery error of about 30 Hz compared with the nominal condition.

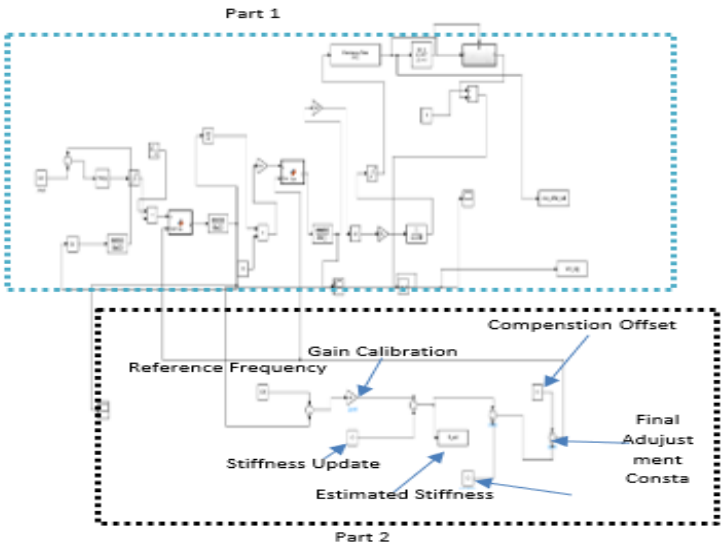

Figure 7: Simulink model of the proposed MEMS gyroscope calibration system showing the stiffness estimation and compensation loop.

Part 1 represent the previously descibed MEMS gyroscope model and VCO-based self-test stages. Part 2 is responsible for implementing the calibration mechanism based on the estimated stiffness variation obtained from the self-test stage. The extracted frequency deviation is processed and converted into an estimated stiffness parameter, which is then used to generate a compensation signal. This compensation is fed back into the system to adjust the degraded parameters and restore the system performance. As a result, the calibration loop enables recovery of the oscillation characteristics, ensuring that the output response closely matches the nominal behavior after degradation.

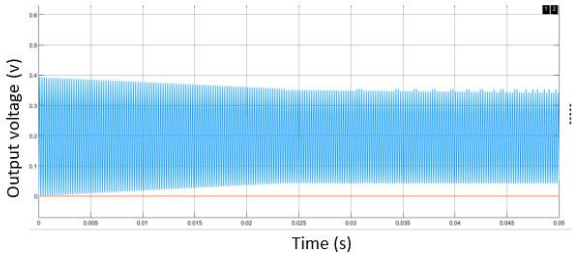

Figure 8: Recovered gyroscope output waveform after adaptive calibration with 95% stiffness restoration.

The adaptive VCO-based calibration loop restored the gyroscope oscillation response after stiffness degradation. The recovered output waveform showed steady periodic behavior while the estimated stiffness reached 95% percent of its nominal value. The proposed method successfully compensates for stiffness variations caused by degradation, enabling the gyroscope performance to remain close. The recovered waveform maintained a stable oscillation response with the calibration frequency approaching the nominal value.

Previous studies on MEMS gyroscope calibration showed recovery rates between 94-95%. The online calibration loop achieved 99.3% stiffness recovery, demonstrates effective restoration and stable adaptive correction capabilities [18].

VIII. Conclusion

This work has created a system that automatically tests itself and calibrates to restore the performance of closed-loop MEMS vibratory gyroscopes which experiences stiffness loss due to parameter changes and aging. The proposed methodology combines a frequency-based self-test mechanism with an online calibration loop to estimate stiffness variation and compensate the degraded response in real time, which showed 99.3% frequency recovery combined with 30 Hz residual error and 95% equivalent stiffness recovery. The recovered response showed clear improvement compared with the degraded case , confirming the effectivenes of the compensation straegy. The results demonstrate that the proposed method functions as a reliable built-in solution which improves reliability to support long-term operational stability of MEMS gyroscopes in real-world sensing applications.

Reference

[1] W. A. Gill, I. Howard, I. Mazhar, and K. McKee, “A Review of MEMS Vibrating Gyroscopes and Their Reliability Issues in Harsh Environments,” Oct. 01, 2022, MDPI. doi: 10.3390/s22197405.

[2] K. Yang, J. Li, J. Yang, and L. Xu, “Research on Adaptive Closed-Loop Control of Microelectromechanical System Gyroscopes under Temperature Disturbance,” Micromachines, vol. 15, no. 9, 2024, doi: 10.3390/mi15091102.

[3] D. Ünsal Öztürk and A. M. Erkmen, “Coriolis Vibratory MEMS Gyro Drive Axis Control with Proxy-Based Sliding Mode Controller,” Micromachines (Basel)., vol. 13, no. 3, Mar. 2022, doi: 10.3390/mi13030446.

[4] Y. Huang, A. Sai Sarathi Vasan, R. Doraiswami, M. Osterman, and M. Pecht, “MEMS reliability review,” 2012. doi: 10.1109/TDMR.2012.2191291.

[5] W. Huang et al., “MEMS and MOEMS Gyroscopes: A Review,” Dec. 01, 2023, Springer Verlag. doi: 10.1007/s13320-023-0693-x.

[6] H. J. Kwon, S. Seok, and G. Lim, “System modeling of a MEMS vibratory gyroscope and integration to circuit simulation,” Sensors (Switzerland), vol. 17, no. 11, Nov. 2017, doi: 10.3390/s17112663.

[7] N. Yazdi, F. Ayazi, and K. Najafi, “Micromachined Inertial Sensors,” 1998.

[8] Z. Instruments, “Control of MEMS Coriolis Vibratory Gyroscopes Application Note Products: HF2PLL, HF2LI-MF, HF2LI-MOD.”

[9] L. Wang, Y. Pan, K. Li, L. He, Q. Wang, and W. Wang, “Modeling and Reliability Analysis of MEMS Gyroscope Rotor Parameters under Vibrational Stress,” Micromachines (Basel)., vol. 15, no. 5, May 2024, doi: 10.3390/mi15050648.

[10] N. Yazdi, F. Ayazi, and K. Najafi, “Micromachined Inertial Sensors,” Proceedings of the IEEE, vol. 86, no. 8, pp. 1640–1659, 1998, doi: 10.1109/5.704269.

[11] L. Wang, Y. Pan, K. Li, L. He, Q. Wang, and W. Wang, “Modeling and Reliability Analysis of MEMS Gyroscope Rotor Parameters under Vibrational Stress,” Micromachines (Basel)., vol. 15, no. 5, May 2024, doi: 10.3390/mi15050648.

[12] K. Yang, J. Li, J. Yang, and L. Xu, “Research on Adaptive Closed-Loop Control of Microelectromechanical System Gyroscopes under Temperature Disturbance,” Micromachines (Basel)., vol. 15, no. 9, Sep. 2024, doi: 10.3390/mi15091102.

[13] J. P. Den Hartog, Mechanical Vibrations. New York: McGraw.Hill, 1985.

[14] D. Schiwietz, E. M. Weig, and P. Degenfeld-Schonburg, “Thermoelastic Damping in MEMS Gyroscopes at High Frequencies,” Jan. 2024, doi: 10.1038/s41378-022-00480-1.

[15] G. Hantos, D. Flynn, and M. P. Y. Desmulliez, “Built-in self-test (Bist) methods for mems: A review,” Jan. 01, 2021, MDPI AG. doi: 10.3390/mi12010040.

[16] T. Xu, X. Xu, J. Zhang, and H. Ye, “Thermal calibration for triaxial gyroscope of MEMS-IMU based on segmented systematic method,” Sci. Rep., vol. 14, no. 1, Dec. 2024, doi: 10.1038/s41598-024-74472-8.

[17] A. S. Ahmed and Q. Al-Gayem, “Three-Axes Mems Calibration Using Kalman Filter and Delaunay Triangulation Algorithm,” Applied Computational Intelligence and Soft Computing, vol. 2023, 2023, doi: 10.1155/2023/7658064.

[18] S. Stančin and S. Tomažič, “Time- and computation-efficient calibration of MEMS 3D accelerometers and gyroscopes,” Sensors, vol. 14, no. 8, pp. 14885–14915, Aug. 2014, doi: 10.3390/s140814885.

[19] M. A. Mohammadi and Q. Al-Gayem, "On-chip self-test solutions for ADC: survey and analysis," IEEE 8th International Conference, 2023.

[20]M. A. Mohammadi and Q. Al-Gayem, "A built-in self-test (BIST) technique for RF transceiver system,"IEEE International Conference on Communications, 2002.